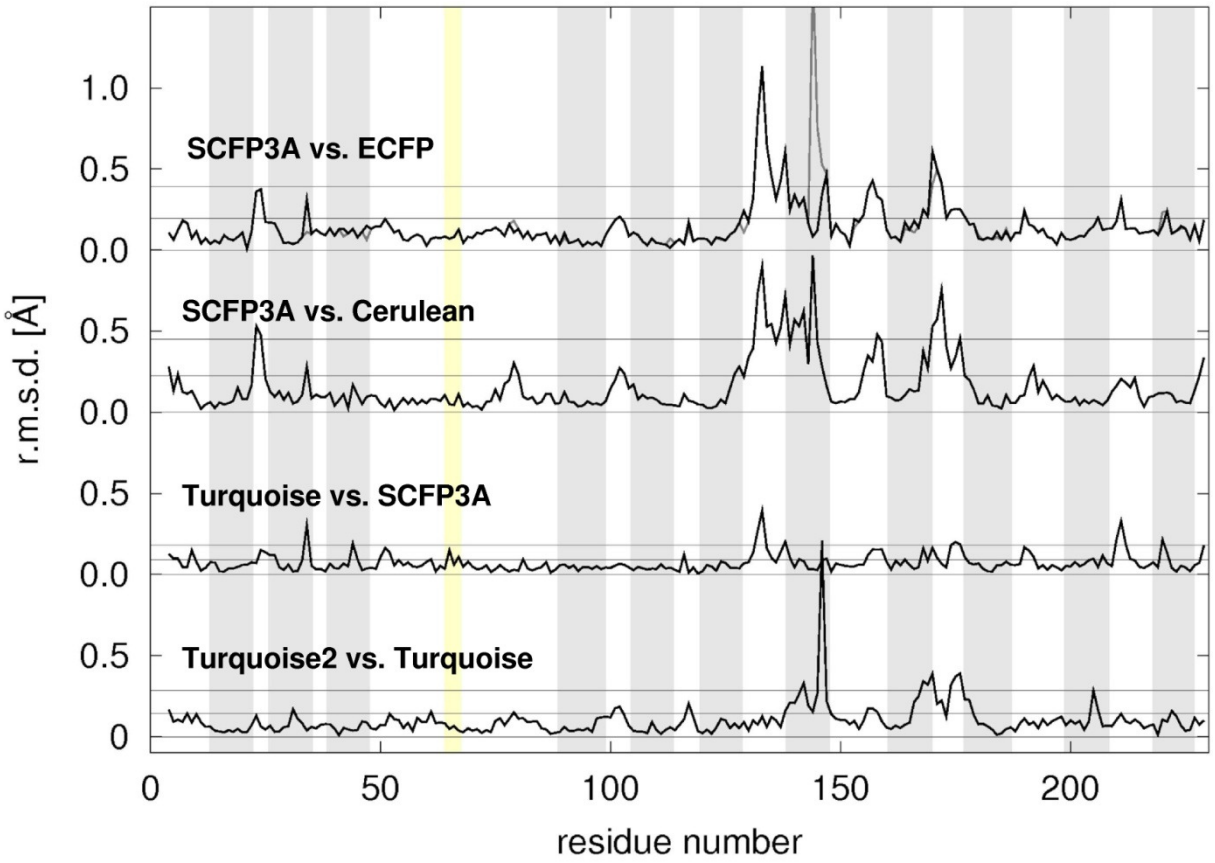

Supplementary Figure S1 | Comparison of main chain atom positions between various pairs of CFP structures. R.m.s.d. (root-mean-square deviation) plots on C_α atoms are represented for various pairs of CFP structures: SCFP3A *vs.* ECFP, SCFP3A *vs.* Cerulean, mTurquoise *vs.* SCFP3A and mTurquoise2 *vs.* mTurquoise (top to bottom)**.** The average r.m.s.d., and twice the average, are represented by two horizontal lines for each alignment. The positions of the eleven β-strands are indicated in grey, and that of the chromophore in yellow.

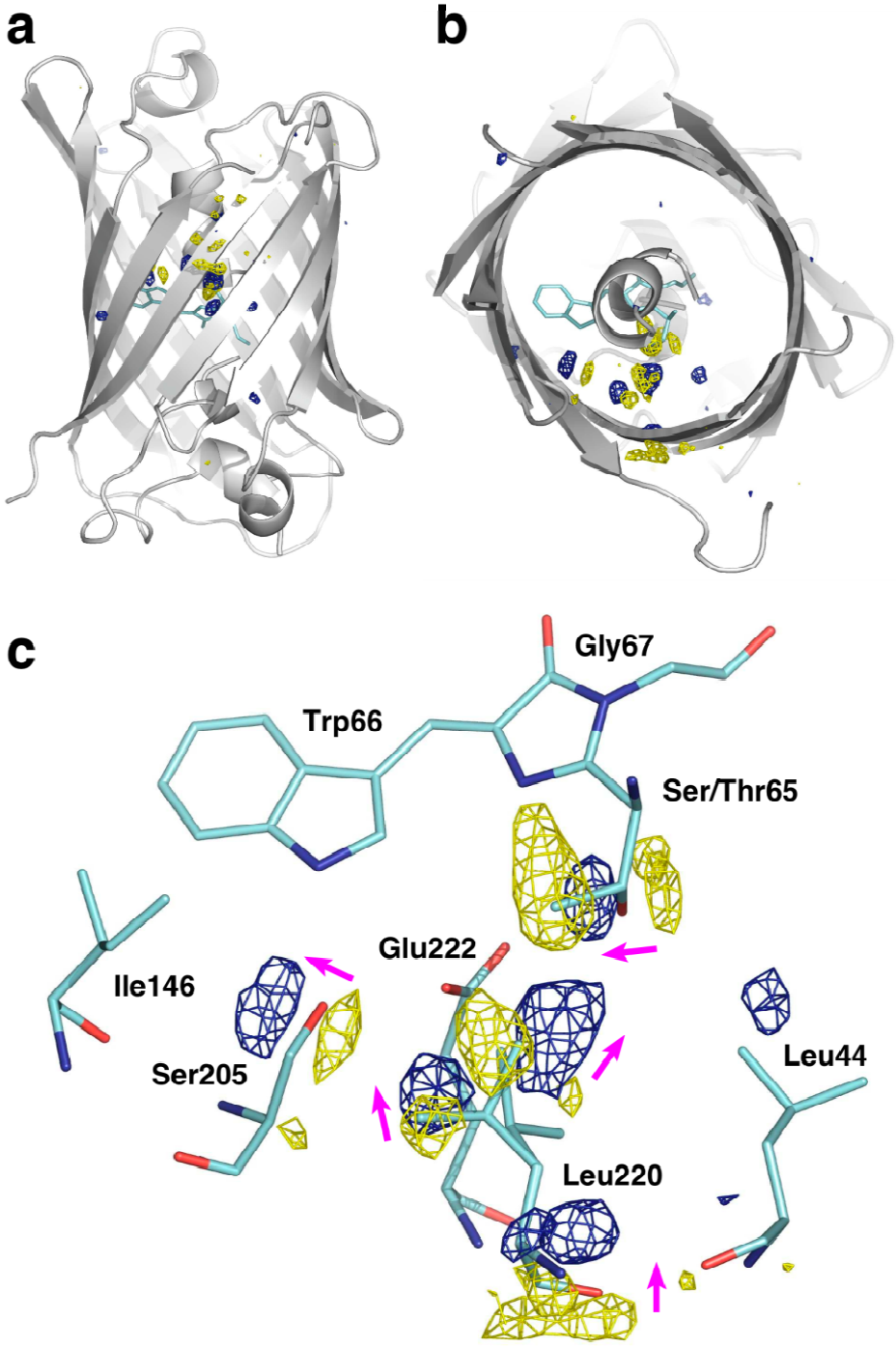

Supplementary Figure S2 | Fourier difference map between mTurquoise and SCFP3A superimposed on the SCFP3A structure. The difference map is contoured at +/- 4.5 σ. Positive and negative peaks are shown in blue and yellow, respectively. (**a**) Overall view from the side of the β-barrel, and (**b**) from top to bottom. (**c**) Close-up on the chromophore region. The strongest peak of the map is on the methyl carbon of Thr65, an atom absent in mTurquoise. Purple arrows indicate atom movements.

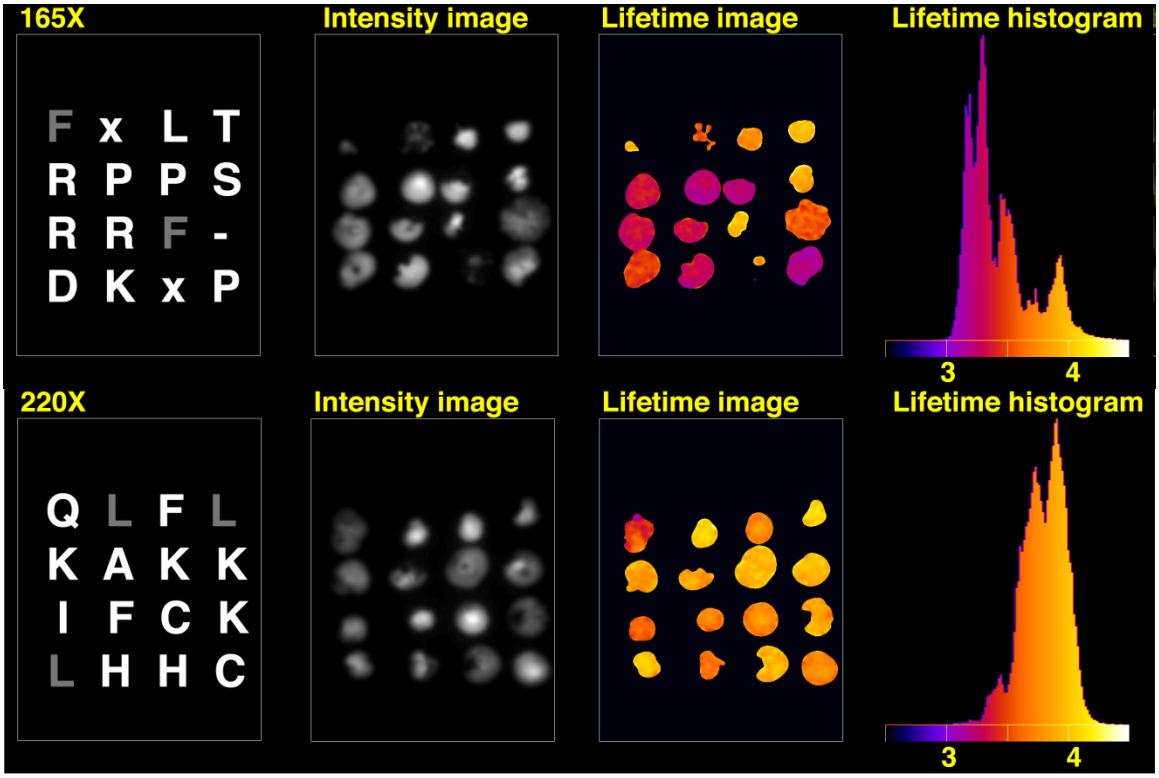

Supplementary Figure S3 | Fluorescence lifetime imaging of bacterial colonies expressing 165X and 220X variants of mTurquoise. FLIM of 165X (upper row) and 220X (lower row), with panels depicting (from left to right) results of the sequencing (the single letter abbreviation amino acids, with the corresponding amino acid in mTurquoise depicted in grey; x indicates that the clone failed to give a readable sequence and - indicates a deletion), fluorescence intensity, the corresponding lifetime map, which is pseudo-colored according to the scale of the lifetime histogram (panel on the right).

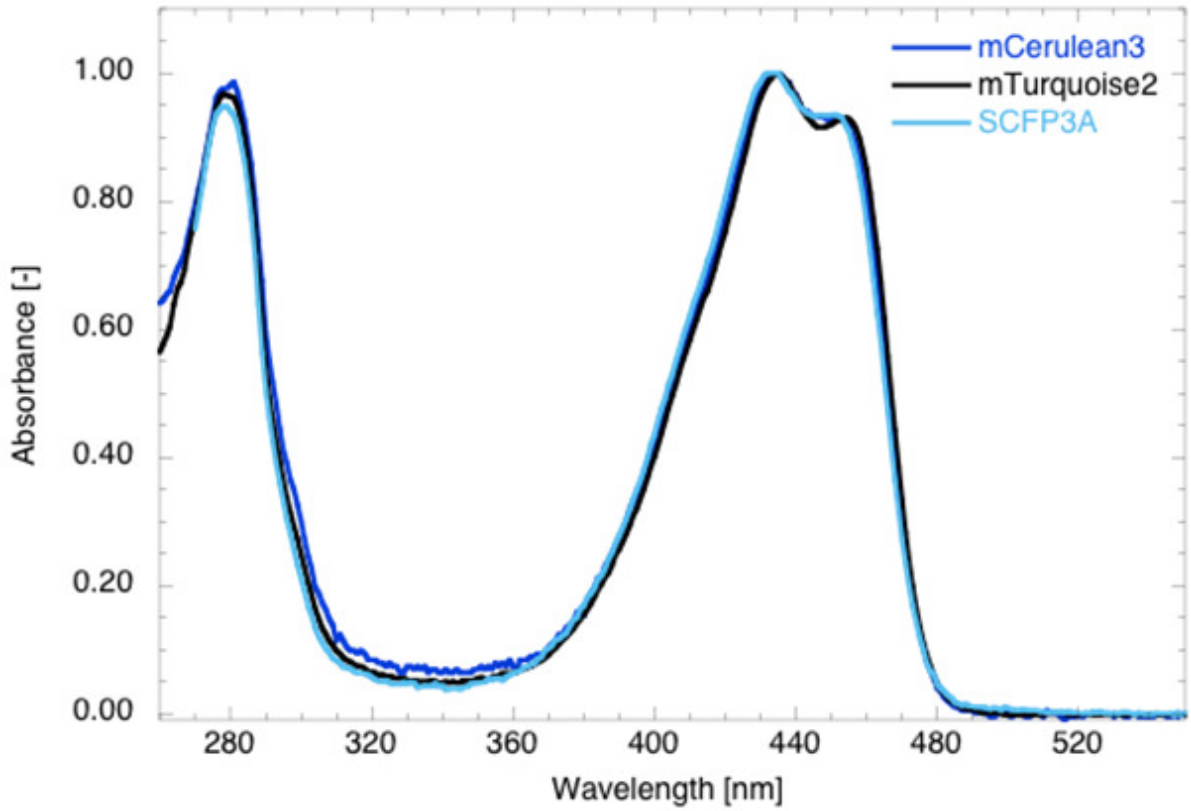

Supplementary Figure S4 | Absorbance spectra of purified CFP variants. The overlay of the absorption spectra of SCFP3A, mTurquoise2 and mCerulean3 shows that the ratio of the absorbance of the chromophore at 434 nm (A_{434}) relative to that of the total protein at 280 nm (A_{280}) is similar among all three variants.

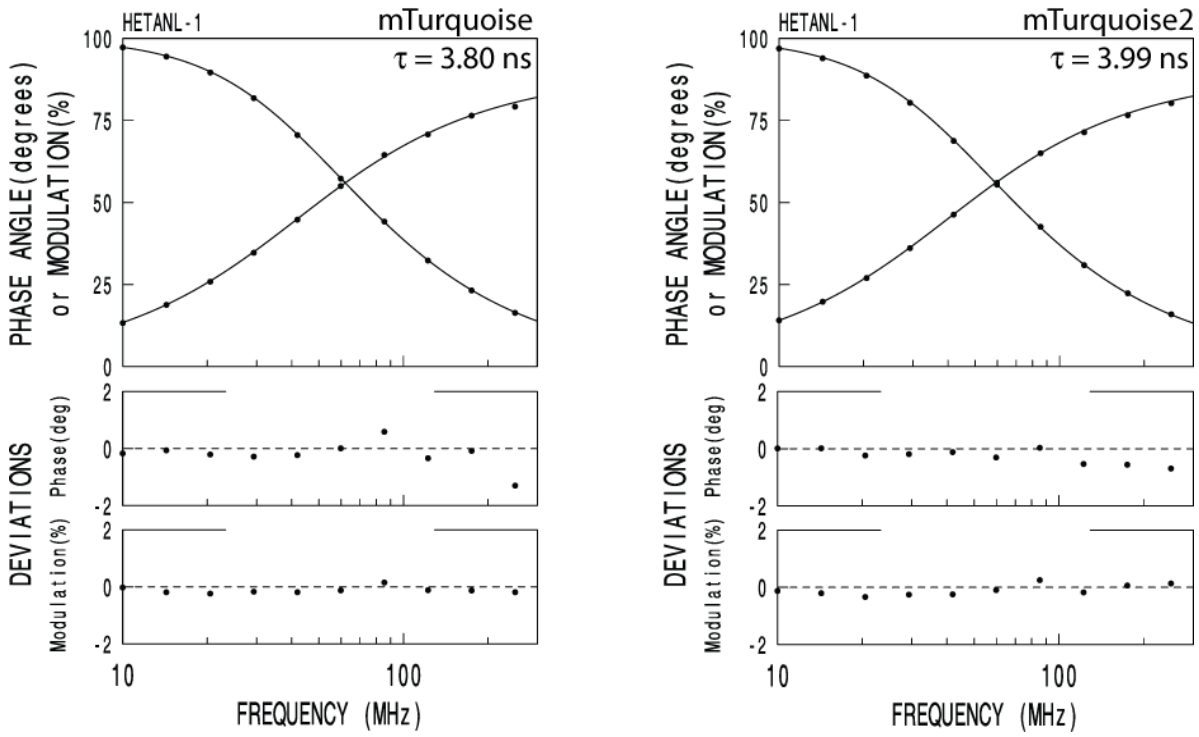

Supplementary Figure S5 | Multifrequency FLIM analysis of living cells expressing mTurquoise variants. Both the data obtained from mTurquoise and mTurquoise2 can be fit with a mono-exponential decay model (indicated by the solid line), yielding a fluorescence lifetime of 3.80 and 3.99 ns, respectively. Data points are the average of three independent measurements of at least two cells.

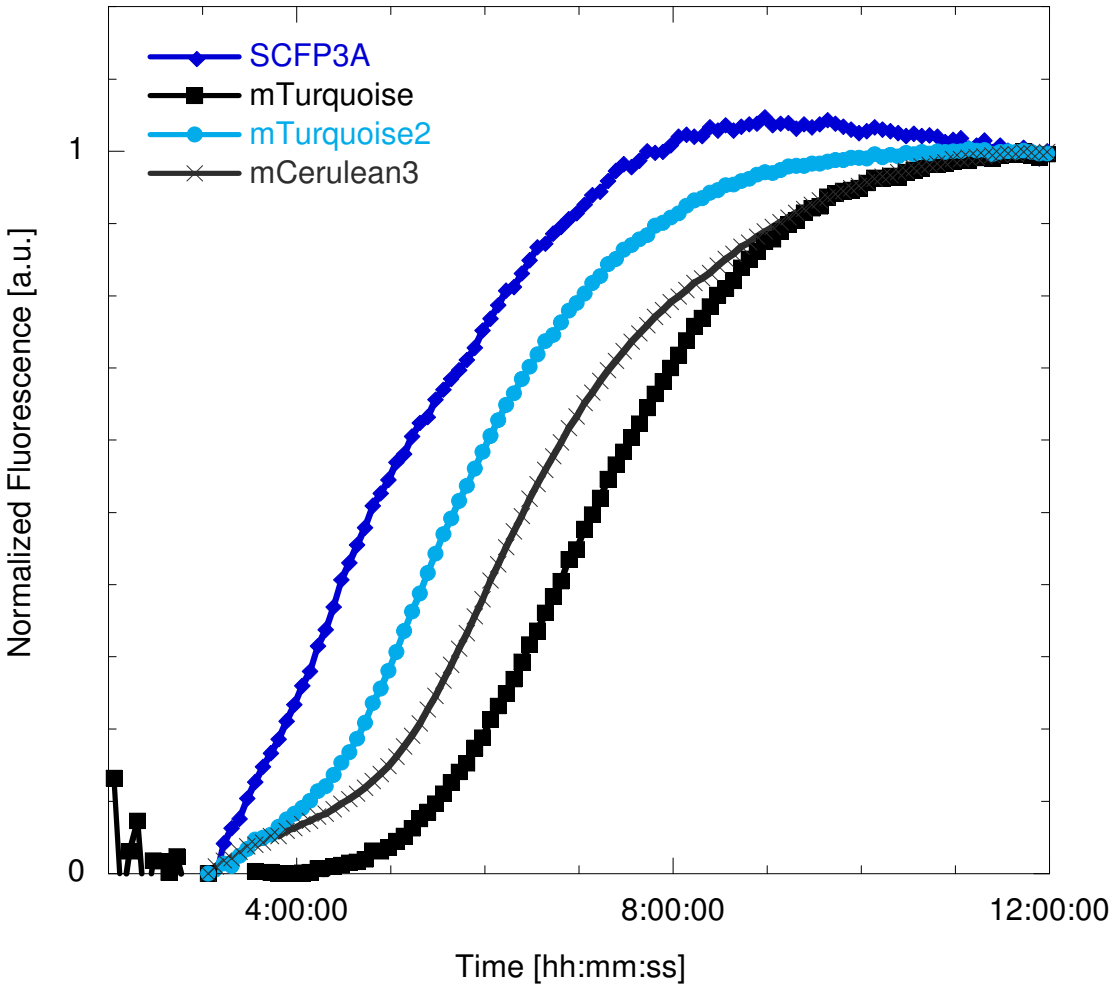

Supplementary Figure S6 | Kinetics of production and maturation of mTurquoise variants in *E. coli*. The experiments were run simultaneously in a 96-well plate reader with fluorescence capabilities. The lines depict the average CFP fluorescence intensity of three wells per CFP variant. The maturation speed of mTurquoise is delayed with respect to SCFP3A by at least one hour, while mTurquoise2 shows a similar maturation rate as SCFP3A.

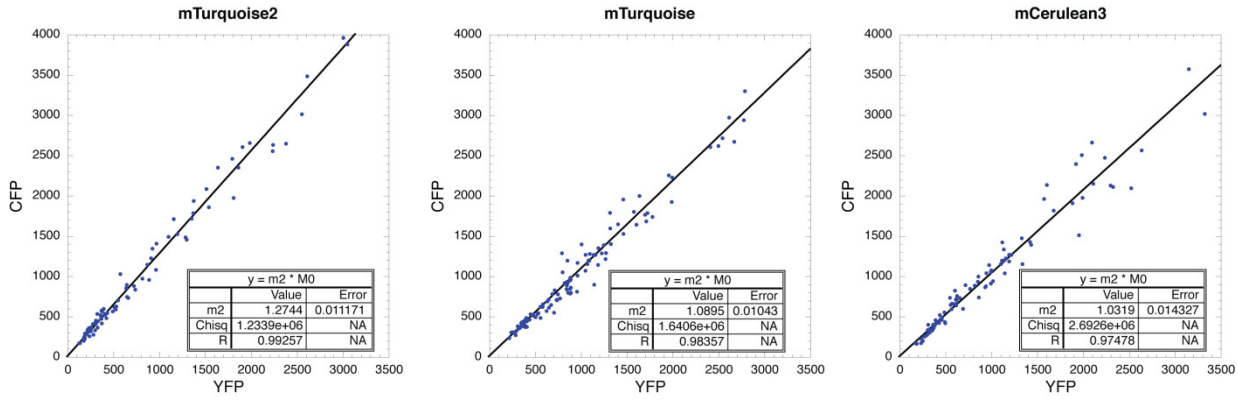

Supplementary Figure S7 | Relative brightness of CFP variants in mammalian cells. HeLa cells were transfected with a construct that drives the simultaneous quantitative co-expression of mTurquoise2, mTurquoise or mCerulean3 and SYFP2. The representative graphs show CFP and YFP intensities quantified on a per-cell basis (each dot is a single cell). The lines represent a linear fit through the single cell data. The slope of the line (m2) determines the brightness *in vivo*, and therefore it can be concluded from this particular experiment that mTurquoise2 is 17% brighter than mTurquoise and 24% brighter than mCerulean3.

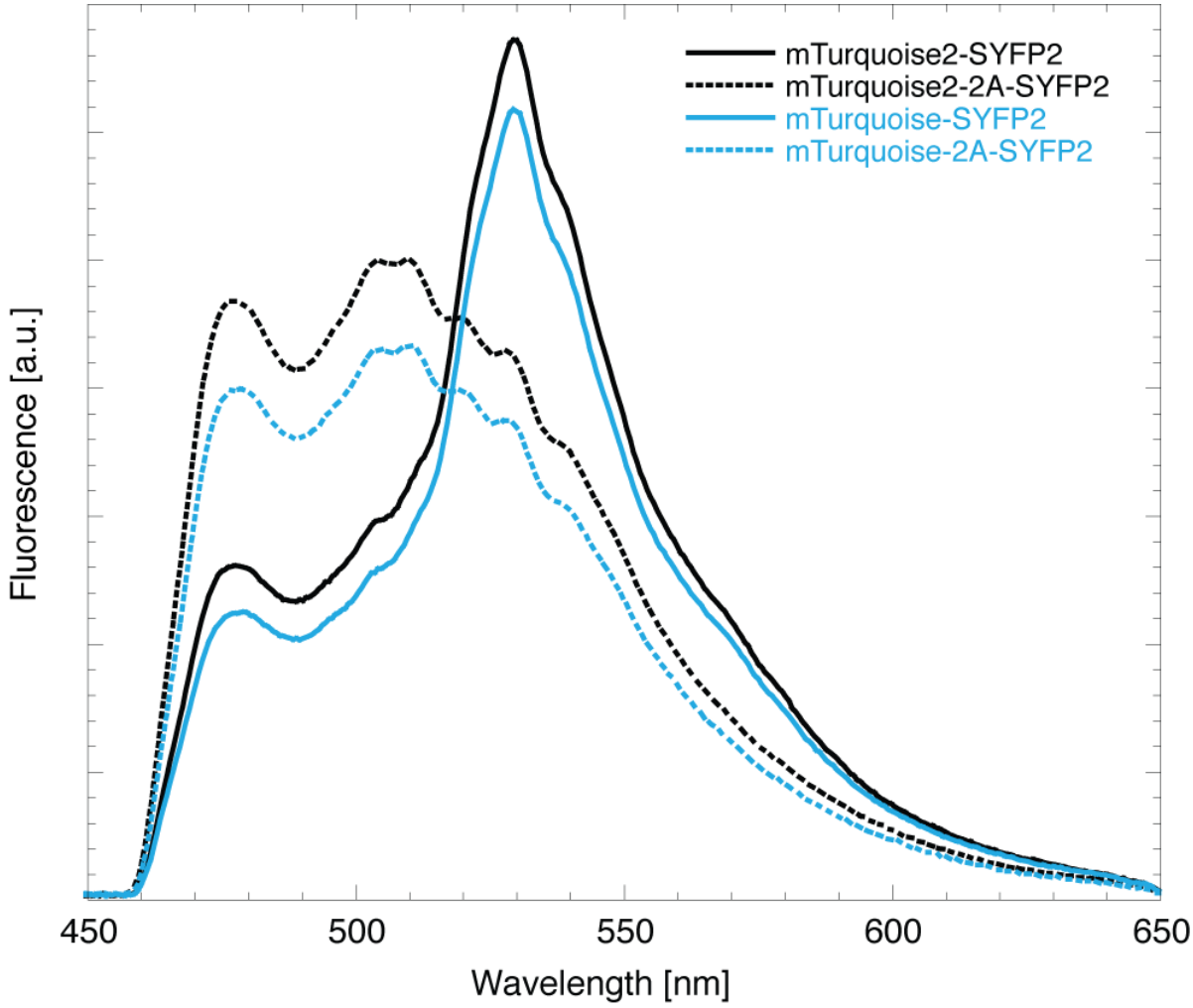

Supplementary Figure S8 | Side-by-side comparison of the mTurquoise-SYFP2 and mTurquoise2-SYFP2 FRET pairs in FRET and a no-FRET situations. Spectral imaging microscopy data from single cells of tandem fusions (FRET, solid lines) are compared to data from single cells co-expressing mTurquoise and SYFP2 at an equimolar level by employing the 2A cleavable peptide (no FRET, dotted lines). Each spectrum is an average from at least 11 cells. Each individual spectrum is normalized for expression level by measuring the YFP intensity.

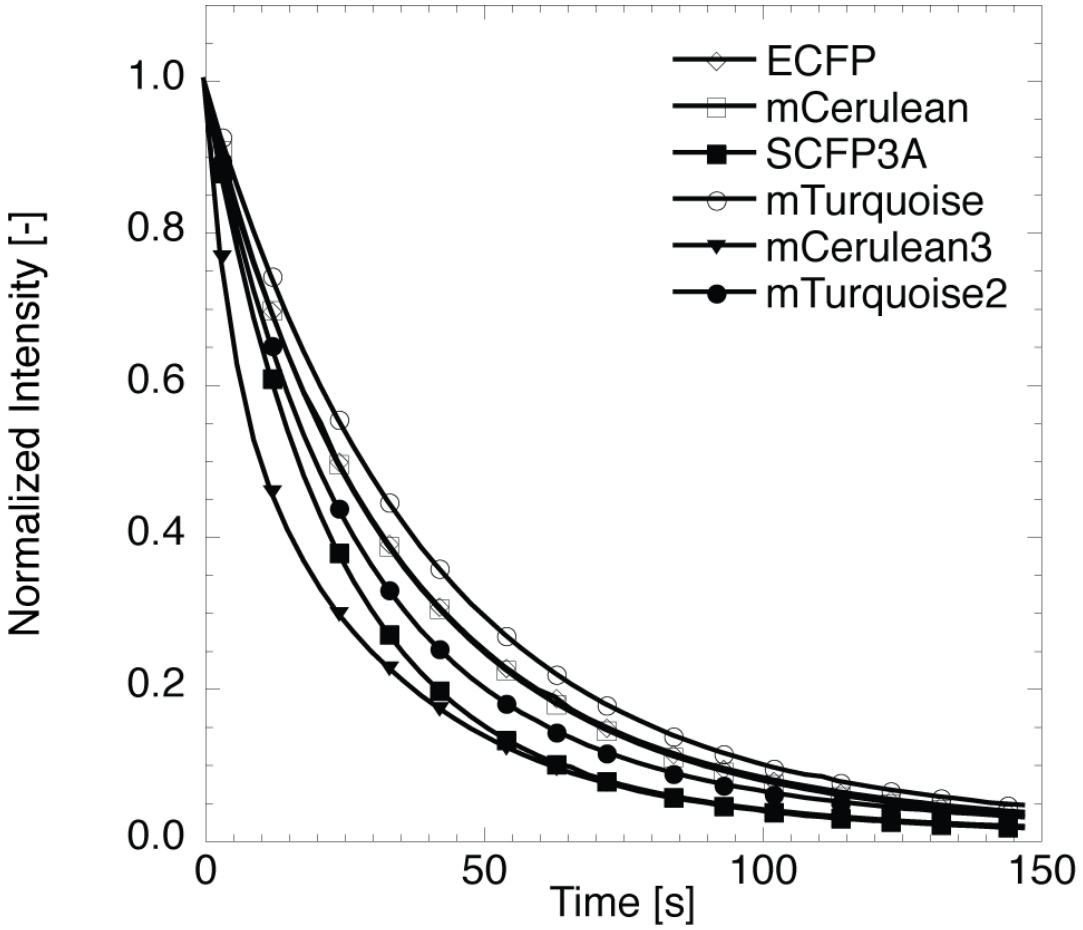

Supplementary Figure S9 | Photostability of CFP variants determined by continuous exposure of living HeLa cells with intense wide-field illumination conditions. The data points are the average of at least 6 cells from 3 independent measurements. Illumination was at 436 nm with an intensity at the objective of 23 W/cm2 (with the 63x objective that was used) (standard error of the mean <2%).

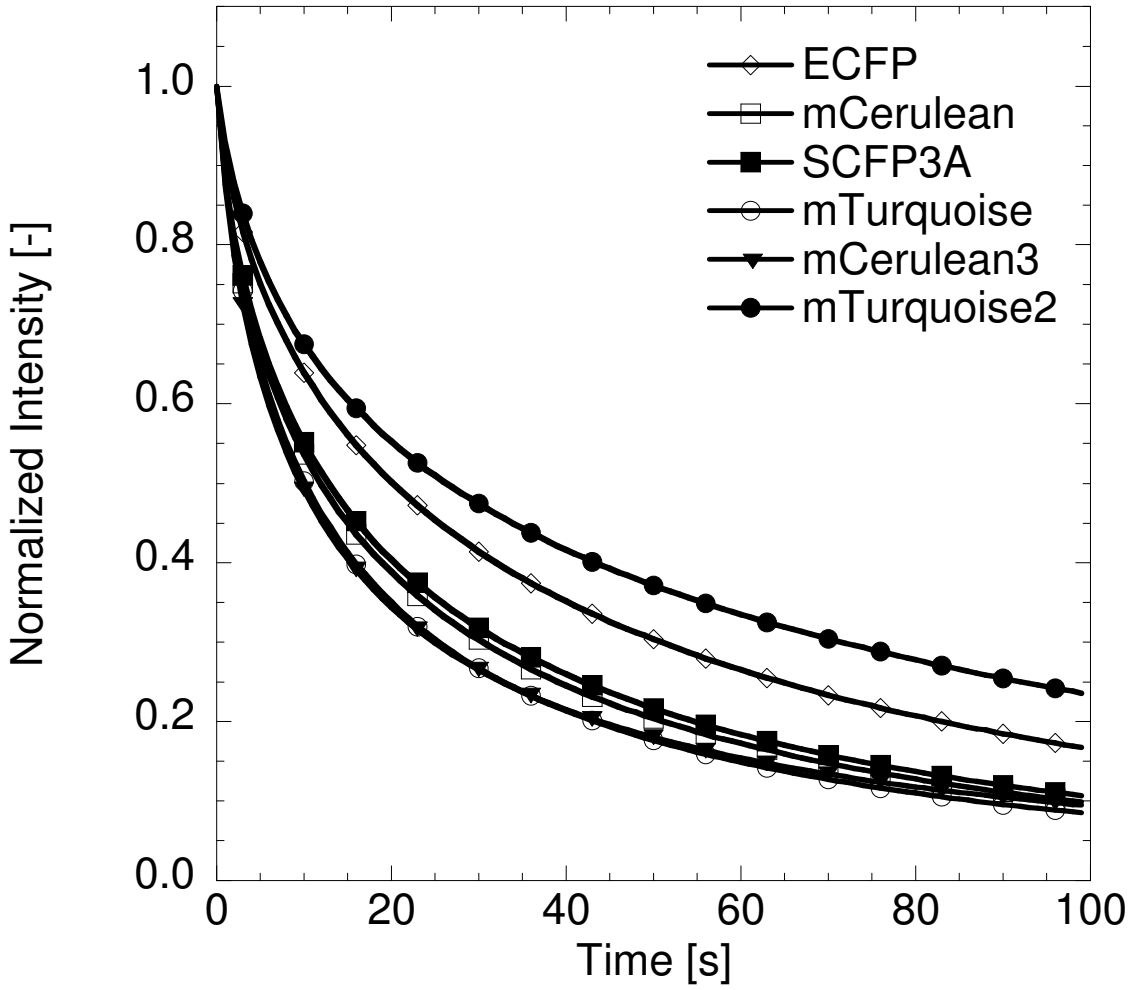

Supplementary Figure S10 | Photostability of CFP variants under laser-scanning conditions. Living HeLa cells expressing CFP-tagged histone 2A were continuously illuminated. Data points are the average of at least 4 cells from 4 independent measurements.

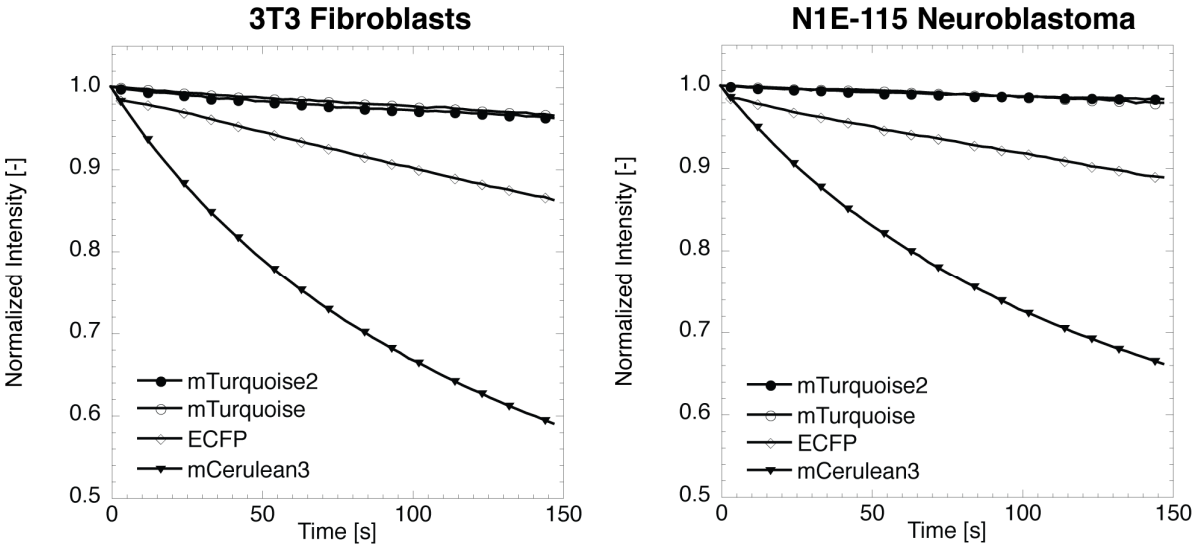

Supplementary Figure S11 | Photostability of mTurquoise2 and CFP variants in different cell types. Photobleaching was measured in 3T3 fibroblasts (1.6 W/cm2) and in N1E-115 neuroblastoma cells (1.4 W/cm2) under wide-field illumination. Data points are average of at least five cells from three independent measurements (standard error of the mean <1%).

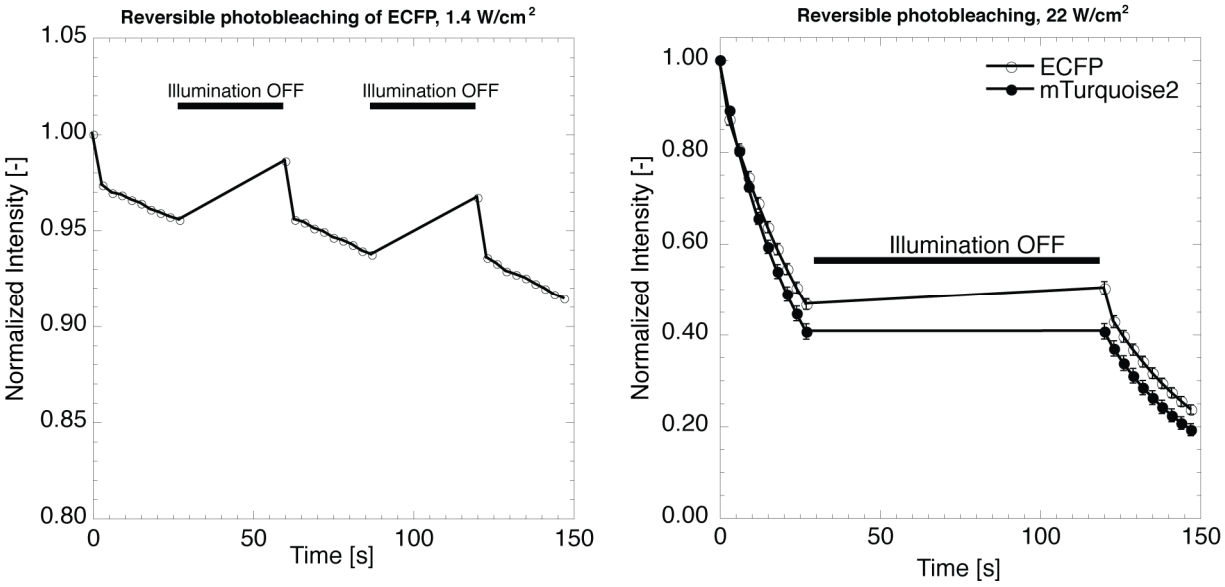

Supplementary Figure S12 | Analysis of reversible photobleaching of ECFP and mTurquoise2 *in vivo*. Cells were irradiated under wide-field illumination for some time after which the excitation was interrupted for some time (indicated by the horizontal bar) to measure potential recovery of reversibly photobleached molecules. ECFP displays about 3% reversible bleaching, while no reversible bleaching was observed for mTurquoise2.

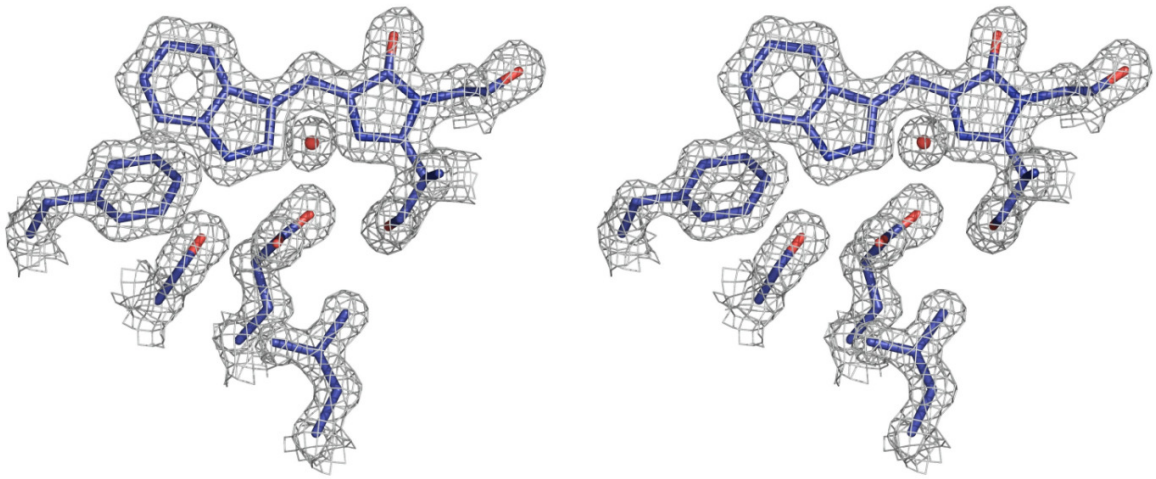

Supplementary Figure S13 | Stereo view of the electron density of the chromophore and neighbouring residues in mTurquoise2. The $2F_o$-F_c map is contoured at a 1.6 σ level around the chromophore (residues 65 to 67) and residues 146, 205, 220 and 222.

Supplementary Table S1 | Mutations present in CFPs mentioned in this work. Mutations introduced for the first time are highlighted in bold.

Residue	ECFP	Cerulean	SCFP3A	mTurquoise	mTurquoise-GL	mTurquoise2
65	T	T	T	**S**	S	S
72	S	A	A	A	A	A
145	Y	**A**	Y	Y	Y	Y
146	I	I	I	I	I	**F**
148	H	**D**	**D**	D	**G**	D
175	S	S	**G**	G	G	G
224	V	V	V	V	**L**	V

Supplementary Table S2 | Ground state (S_0) interaction energies. Interaction energies are calculated between pairs of side chains of equivalent residues in SCFP3A, mTurquoise and mTurquoise2, in the structures which have been energy-minimized in the S_0 state.

	SCFP3A	mTurquoise	**mTurquoise – SCFP3A**	mTurquoise2	**mTurquoise2 – mTurquoise**
Residue 65					
Res65/Glu222	-43.00[a]	-45.83	**-2.83**	-47.92	**-2.09**
Res65/Leu220	-0.62	-2.90	**-2.28**	-3.23	**-0.33**
Glu222/Leu220	-7.73	-7.59	**0.14**	-8.76	**-1.17**
Ser205					
Ser205/Leu220	-1.10	-1.63	**-0.53**	-1.43	**0.20**
Ser205/Glu222	-57.89	-57.34	**0.55**	-54.25	**3.09**
Ser205/Res146	-0.75	-1.64	**-0.89**	-4.64	**-3.00**
Ser205/Trp66	-23.70	-24.90	**-1.20**	-23.07	**1.83**
H-bond	*-19.98*	*-21.18*	***-1.20***	*-18.16*	***3.02***
Trp66					
Trp66/Glu222	-0.73	-1.53	**-0.80**	-2.90	**-1.37**
Trp66/Res65	-1.44	-0.62	**0.82**	-0.68	**-0.06**
Trp66/Ser147	0.14	-0.60	**-0.74**	-0.13	**0.47**
Trp66/Asp148	-3.31	-3.39	**-0.08**	-1.89	**1.50**
Trp66/Val150	-2.65	-1.78	**0.87**	-1.72	**0.06**
Trp66/Phe165	-10.55	-10.86	**-0.31**	-10.94	**-0.08**
Trp66/Ile167	-4.72	-3.63	**1.09**	-4.48	**-0.85**
Trp66/Val61	-2.70	-2.73	**-0.03**	-2.94	**-0.21**
Trp66/Thr62	-12.44	-13.30	**-0.86**	-11.57	**1.73**
Trp66/Thr203	-6.90	-7.29	**-0.39**	-6.86	**0.43**
Residue 146					
Res146/Trp66	-4.07	-3.92	**0.15**	-10.69	**-6.77**
Res146/Ile167	-5.99	-4.99	**1.00**	-9.61	**-4.62**
Res146/Val61	-5.52	-4.36	**1.16**	-4.64	**-0.28**
Res146/Thr62	-1.75	-2.17	**-0.42**	-3.06	**-0.89**
Sum			**-5.58**		**-12.41**

[a]Expressed in $kJ \cdot mol^{-1}$

Supplementary Table S3 | Excited state (S_1) interaction energies ('vertical excitation' case). Interaction energies are calculated between pairs of side chains of equivalent residues in SCFP3A, mTurquoise and mTurquoise2, in the structures which have been energy-minimized in the S_0 state with excited state charges.

	SCFP3A	mTurquoise	**mTurquoise – SCFP3A**	mTurquoise2	**mTurquoise2 – mTurquoise**
Residue 65					
Res65/Glu222	-43.06	-45.94	**-2.88**	-47.99	**-2.05**
Res65/Leu220	-0.62	-2.90	**-2.28**	-3.23	**-0.33**
Glu222/Leu220	-7.73	-7.59	**0.14**	-8.76	**-1.17**
Ser205					
Ser205/Leu220	-1.10	-1.63	**-0.53**	-1.43	**0.20**
Ser205/Glu222	-57.89	-57.34	**0.55**	-54.25	**3.09**
Ser205/Res146	-0.75	-1.64	**-0.89**	-4.64	**-3.00**
Ser205/Trp66	-27.76	-29.19	**-1.43**	-27.28	**1.91**
H-bond	*-28.60*	*-30.53*	***-1.93***	*-26.84*	***3.69***
Trp66					
Trp66/Glu222	12.44	9.34	**-3.10**	7.33	**-2.01**
Trp66/Res65	-0.57	0.27	**0.84**	0.29	**0.02**
Trp66/Ser147	0.38	-0.04	**-0.42**	0.37	**0.41**
Trp66/Asp148	-8.35	-8.16	**0.19**	-7.65	**0.51**
Trp66/Val150	-2.75	-1.89	**0.86**	-1.81	**0.08**
Trp66/Phe165	-10.97	-10.93	**0.04**	-11.83	**-0.90**
Trp66/Ile167	-4.67	-3.59	**1.08**	-4.44	**-0.85**
Trp66/Val61	-2.49	-2.53	**-0.04**	-2.74	**-0.21**
Trp66/Thr62	-11.89	-12.11	**-0.22**	-10.99	**1.12**
Trp66/Thr203	-4.04	-4.46	**-0.42**	-4.43	**0.03**
Residue 146					
Res146/Trp66	-4.00	-3.87	**0.13**	-10.56	**-6.69**
Res146/Ile167	-5.99	-4.99	**1.00**	-9.61	**-4.62**
Res146/Val61	-5.52	-4.36	**1.16**	-4.64	**-0.28**
Res146/Thr62	-1.75	-2.17	**-0.42**	-3.06	**-0.89**
Sum			**-6.64**		**-15.63**

[a]Expressed in $kJ \cdot mol^{-1}$

Supplementary Table S4 | Excited state (S_1) interaction energies ('excited-state relaxation' case). Interaction energies between pairs of side chains of equivalent residues in SCFP3A, mTurquoise and mTurquoise2, in the structures which have been energy-minimized in the S_1 state.

	SCFP3A	mTurquoise	**mTurquoise – SCFP3A**	mTurquoise2	**mTurquoise2 – mTurquoise**
Residue 65					
Res65/Glu222	-43.18	-45.58	**-2.40**	-47.74	**-2.16**
Res65/Leu220	-0.70	-2.92	**-2.22**	-3.24	**-0.32**
Glu222/Leu220	-7.74	-7.61	**0.13**	-8.89	**-1.28**
Ser205					
Ser205/Leu220	-1.12	-1.54	**-0.42**	-1.46	**0.08**
Ser205/Glu222	-58.14	-57.47	**0.67**	-54.67	**2.80**
Ser205/Res146	-0.69	-1.62	**-0.93**	-4.59	**-2.97**
Ser205/Trp66	-27.69	-29.08	**-1.39**	-26.62	**2.46**
H-bond	*-28.48*	*-30.24*	***-1.76***	*-25.93*	***4.31***
Trp66					
Trp66/Glu222	11.79	8.69	**-3.10**	6.15	**-2.54**
Trp66/Res65	-0.59	0.21	**0.80**	0.30	**0.09**
Trp66/Ser147	0.36	-0.05	**-0.41**	0.36	**0.41**
Trp66/Asp148	-8.31	-8.15	**0.16**	-7.66	**0.49**
Trp66/Val150	-2.76	-1.94	**0.82**	-1.97	**-0.03**
Trp66/Phe165	-10.97	-10.97	**0.00**	-11.77	**-0.80**
Trp66/Ile167	-4.66	-3.69	**0.97**	-4.44	**-0.75**
Trp66/Val61	-2.48	-2.48	**0.00**	-2.81	**-0.33**
Trp66/Thr62	-11.95	-12.15	**-0.20**	-10.91	**1.24**
Trp66/Thr203	-4.00	-4.80	**-0.80**	-4.71	**0.09**
Residue 146					
Res146/Trp66	-4.00	-3.88	**0.12**	-10.73	**-6.85**
Res146/Ile167	-6.00	-5.01	**0.99**	-9.53	**-4.52**
Res146/Val61	-5.52	-4.39	**1.13**	-4.67	**-0.28**
Res146/Thr62	-1.74	-2.10	**-0.36**	-3.08	**-0.98**
Sum			**-6.44**		**-16.15**

[a]Expressed in $kJ \cdot mol^{-1}$

Supplementary Table S5 | Total number of emitted photons per single CFP molecule before photobleaching. Bleach rates were calculated from data presented in **Fig. 6h** and **Supplementary Figure S9**.

CFP variant	QY	Bleach rate k_{bl} (10^{-3}/s)		N_{em} (10^6/molecule)	
		23 W/cm^2	1.6 W/cm^2	23 W/cm^2	1.6 W/cm^2
mTurquoise2	0.93	34.9	0.23	0.15	1.62
mTurquoise	0.84	24.6	0.21	0.20	1.61
SCFP3A	0.56	40.2	0.50	0.08	0.45
mCerulean3	0.80	77.3	4.76	0.06	0.07
mCerulean	0.49	30.3	0.66	0.09	0.30
ECFP	0.36	34.3	0.89	0.06	0.16

Supplementary Table S6 | Primers used in this study.

Name	Type	Sequence[a]
146X-forward	Mutagenesis	ctggagtacaactacNNKagcgacaacgtctat
146X-reverse	Mutagenesis	atagacgttgtcgctMNNgtagttgtactccag
165X-forward	Mutagenesis	ggcatcaaggccaacNNKaagatccgccacaac
165X-reverse	Mutagenesis	gttgtggcggatcttMNNgttggccttgatgcc
220X-forward	Mutagenesis	cgcgatcacatggtcNNKctggagttcgtgacc
220X-reverse	Mutagenesis	ggtcacgaactccagMNNgaccatgtgatcgcg
206A-forward	Mutagenesis	cctgagcacccagtccGCCctgagcaaagacccc
206A-reverse	Mutagenesis	ggggtctttgctcagGGCggactgggtgctcagg

[a]N=A,C,G,T; K=G,T; M=A,C

Supplementary Table S7 | Ground state (S_0) atomic charges. Atomic charges of the chromophore obtained from the OPLS-AA force field are compared with those calculated at the RHF/6-31G* level by the RESP method (values reported in atomic units).

Atom	OPLS-AA	RESP(RHF/6-31G*)
Thr65 part (SCFP3A)		
N1	-0.50000	-0.41570
H1	0.30000	0.27190
CA1	0.14000	-0.03273
HA1	0.06000	0.09196
CB1	0.14000	0.35661
HB1	0.06000	-0.02332
CG2	-0.18000	-0.24863
HG21	0.06000	0.06948
HG22	0.06000	0.06948
HG23	0.06000	0.06948
OG1	-0.68300	-0.64716
HG1	0.41800	0.41580
Ser65 part (mTurquoise)		
N1	-0.50000	*n/a*
H1	0.30000	*n/a*
CA1	0.14000	*n/a*
HA1	0.06000	*n/a*
CB1	0.08000	*n/a*
HB1	0.06000	*n/a*
HB2	0.06000	*n/a*
OG1	-0.68300	*n/a*
HG1	0.41800	*n/a*
Imidazolinone ring		
C1	0.29500	0.29637
N2	-0.49000	-0.21691
N3	-0.20000	-0.31807
C2	0.50000	0.58114
O2	-0.50000	-0.55726
CA2	0.31000	-0.10130
Methylene bridge		
CB	-0.11500	-0.13672
HB	0.11500	0.14281
Indole ring		
CG	0.02500	0.03980
CD1	-0.11500	-0.14575
HD1	0.11500	0.21142
NE1	-0.57000	-0.36993
HE1	0.42000	0.36616
CE2	0.13000	0.14055
CZ2	-0.11500	-0.25499
HZ2	0.11500	0.16315
CH2	-0.11500	-0.13566
HH2	0.11500	0.14880
CZ3	-0.11500	-0.23503
HZ3	0.11500	0.15561
CE3	-0.11500	-0.06659
HE3	0.11500	0.05953
CD2	-0.05500	0.04436
Gly67 part		
CA3	0.08000	0.00444
HA31	0.06000	0.10397
HA32	0.06000	0.07353
C3	0.50000	0.59730
O3	-0.50000	-0.56790

Supplementary Table S8 | Atomic charge variations between ground (S_0) and excited (S_1) states. Changes of electron density are calculated on the atoms of the chromophore upon excitation from the S_0 state to the S_1 state (values reported in atomic units).

Atom	SCFP3A	mTurquoise	mTurquoise2
Thr65 part (SCFP3A)			
N1	-0.00160		
H1	-0.00034		
CA1	0.00027		
HA1	0.00016		
CB1	-0.00009		
HB1	0.00007		
CG2	0.00009		
HG21	0.00001		
HG22	0.00000		
HG23	0.00002		
OG1	0.00006		
HG1	0.00000		
Ser65 part (mTurquoise)			
N1		-0.00103	-0.00161
H1		-0.00029	-0.00034
CA1		0.00050	0.00025
HA1		0.00027	0.00019
CB1		0.00004	0.00000
HB1		0.00004	0.00003
HB2		0.00001	0.00001
OG1		0.00022	0.00013
HG1		-0.00000	0.00000
Imidazolinone ring			
C1	-0.02464	-0.01892	-0.02404
N2	-0.00127	0.01540	0.00525
N3	0.02185	0.02716	0.02225
C2	-0.09142	-0.09320	-0.08796
O2	-0.01400	-0.01618	-0.01606
CA2	0.14565	0.11691	0.13311
Methylene bridge			
CB	-0.26429	-0.25981	-0.26341
HB	-0.00005	0.00006	-0.00002
Indole ring			
CG	0.21670	0.21077	0.21627
CD1	-0.08776	-0.08526	-0.08936
HD1	-0.00016	-0.00012	-0.00010
NE1	0.06829	0.06984	0.06803
HE1	-0.00007	-0.00004	-0.00014
CE2	-0.01866	-0.01827	-0.01846
CZ2	0.03272	0.02962	0.03536
HZ2	-0.00000	-0.00000	0.00000
CH2	0.01709	0.01915	0.01799
HH2	-0.00000	-0.00000	0.00000
CZ3	-0.01018	-0.01152	0.01041
HZ3	-0.00000	0.00000	0.00000
CE3	0.04657	0.04759	0.04870
HE3	-0.00000	-0.00000	0.00000
CD2	-0.03499	-0.03325	-0.03584

Supplementary Note 1

Interaction energy calculation details

pK_a of titratable residues in SCFP3A, mTurquoise and mTurquoise2 were calculated on the H++ web server[37], and protonation states were then deduced at pH 7.0. The hydrogen bond network of the protonated protein models was optimized with the water molecules observed in the X-ray structures, using the PDB2PQR program[38]. The chromophore was explicitly taken into account in both pK_a and hydrogen bond network calculations. All subsequent steps were carried out with the fDynamo library[35]. The protonated models were placed in a pre-equilibrated box of water molecules and sodium ions. The OPLS-AA (Optimized Potentials for Liquid Simulations – All Atoms) force field was applied to the protein[36], while the TIP3P model was used for the water molecules[39]. Parameters for the chromophore were derived from those of the corresponding three amino acids in the OPLS-AA force field. Charges of the OPLS-AA force field are in good agreement with those reported in the literature by the RESP method, which relies on an electrostatic potential of RHF/6-31G* level[40] (**Supplementary Table S7**). Atomic positions of the protein were optimized by using a conjugate gradient algorithm with an integration step of 10^{-3} Å, until the root mean square of the force components reached 10^{-1} $kJ \cdot mol^{-1} \cdot Å^{-1}$. Interaction energies between residue side chains were calculated in the ground state (S_0), by adding electrostatic and vdW terms of the OPLS-AA force field.

Photo-induced changes of electron density on the chromophore in the excited state (S_1) were calculated with a hybrid quantum mechanical/molecular mechanical (QM/MM) potential[35]. The PDDG-PM3 semi-empirical method[41] was used in combination with a configuration interaction ([10,10]-CISD) wave function to describe the electron density of the chromophore. Remaining atoms of the system were treated with the OPLS-AA force field. Energy-minimization of the solvated protein in its ground state S_0 was performed using a criterion of convergence equal to 1 $kJ \cdot mol^{-1} \cdot Å^{-1}$ for the conjugate gradient algorithm. The electron density was then calculated in both S_0 and S_1 states for further population analysis. Calculated differences between Löwdin atomic charges of both electronic states are reported in **Supplementary Table S8**. The variations of the atomic charges are consistent with the intramolecular charge transfer reported in the literature[42] and essentially consist in the build-up of partial charges on the three atoms of the methylene bridge between the two rings of the chromophore: a negative one on atom CB, and two positive ones on atoms CA2 and CG. The obtained electron density differences were added to the OPLS-AA atomic charges in order to model the excited state S_1 of both proteins. The resulting force field was used to calculate the

S_1 interaction energies between side chains of residues in the S_0 energy-minimized geometry ('vertical excitation' case, **Supplementary Table S3**, which can be compared to the ground state case, **Supplementary Table S2**). The same force field was used to perform an energy-minimization of the S_0 energy-minimized structures, resulting in S_1 energy-minimized structures. Interactions energies were then calculated in the latter geometry, which corresponds to the 'excited state relaxation' case (**Supplementary Table S4**). Results similar to those of vertical excitation were observed.

Variations in chromophore interactions: SCFP3A vs. mTurquoise

The T65S mutation primarily strengthens the already very strong H-bond-mediated interaction between residue 65 and Glu222. Additionally, room created by the loss of the methyl group allows a vdW interaction to occur between Thr/Ser65 and Leu220 (-2.9 $kJ \cdot mol^{-1}$ in mTurquoise *vs.* -0.6 $kJ \cdot mol^{-1}$ in SCFP3A). The consequence of this interaction is the displacement of Leu220 towards Ser205 with conservation of the vdW interaction. Relocation of the Ser205 side chain has several key consequences, the least being the conserved strong interaction with Glu222. It also establishes a mild vdW contact with Ile146 through its carbonyl group which is barely present in SCFP3A (-1.6 $kJ \cdot mol^{-1}$ in mTurquoise *vs.* -0.7 $kJ \cdot mol^{-1}$ in SCFP3A). Finally, and most importantly, a strong increase in stabilization occurs between Ser205 and the indole ring of Trp66 which are engaged in the only H-bond stabilizing the chromophore: atoms engaged in this H-bond are stabilized by -1.9 $kJ \cdot mol^{-1}$ in the excited state of mTurquoise, which leads to an overall chromophore stabilization of -1.4 $kJ \cdot mol^{-1}$ by Ser205. This is accompanied by an even larger gain of stabilization of Glu222 by -3.1 $kJ \cdot mol^{-1}$ in the excited state. This comes at the cost of a limited destabilization of the chromophore by residues on the other side of the chromophore (essentially by the pair of residues Val150 and Phe165), but the overall interaction energy is increased. The great importance of this H-bond on the fluorescence properties of the tryptophan-based chromophore is backed up by our observation that a S205A mutant of the CFP variant Cerulean has a QY of only 0.17, which means that the loss of the chromophore-stabilizing H-bond results in almost a 3-fold decrease of the fluorescence QY.

Variations in chromophore interactions: mTurquoise vs. mTurquoise2

The first effect of the I146F mutation is to double the vdW interaction energy between residue 146 and the surrounding residues 61, 62, 66 and 167 (-28 $kJ \cdot mol^{-1}$ *vs.* -15 $kJ \cdot mol^{-1}$) *via* their respective side chains. Additionally, residue 146 establishes a much stronger vdW interaction

with Ser205 *via* its carbonyl group in mTurquoise2 (-5 kJ·mol^{-1} *vs.* -2 kJ·mol^{-1}). As a consequence, this creates an anchoring point for the seventh strand inside the protein core which constitutes a sound explanation for its stabilization.

We observe in mTurquoise2 that the H-bond between Ser205 and Trp66 is weakened compared to mTurquoise. This can be explained by the balance of interactions with Glu222 and Ile146, which are tuned by the mutations T65S (in mTurquoise) and I146F (in mTurquoise2) at the two opposite sides of the chromophore. The optimal orientation of the H-bond is reached in mTurquoise, when the interaction with Ile146 is mild. This apparent loss of stabilization is, however, much more than compensated by the increase of stabilization by Phe146 (see above).

Finally, in mTurquoise2, Glu222 is found to engage more stable interactions with two residues of the chromophore, Ser65 and Trp66 in the excited state (by -2 kJ·mol^{-1} each). Noteworthy, the Trp66-Glu222 interaction is highly repulsive in the excited state of SCFP3A (12 kJ·mol^{-1}) due to a charge transfer on the methylene bridge of the chromophore (change of 0.26 atomic units on atom CB, see **Supplementary Table S8**). This repulsive interaction is progressively attenuated in mTurquoise (9 kJ·mol^{-1}) and then in mTurquoise2 (7 kJ·mol^{-1}). These two enhanced interactions with the chromophore also contribute to the improvement of the fluorescent properties.

Supplementary Note 2

Calculation of emitted photons by CFPs before irreversible bleaching

The calculation of emitted photons before photobleaching is calculated from the initial rate of photobleaching, the absorption cross section of a CFP molecule and the power of the employed excitation light. The absorption cross section σ (units cm^2/molecule) of a CFP molecule is given by[43]

$$\sigma = \frac{1000 \ln 10 \, \varepsilon}{N_A} \qquad \text{(S1)}$$

where ε is the extinction coefficient at the employed excitation wavelength (units $M^{-1} \cdot cm^{-1}$) and N_A is Avogadro's number (number of molecules per mole).

The excitation power density W (units W/cm^2) is related to the excitation photon flux Ψ (units photons $cm^{-2} \cdot s^{-1}$) according to:

$$\Psi = \frac{W \lambda}{h c} \qquad \text{(S2)}$$

Where λ is the wavelength (units m) of excitation, h is Planck's constant and c is the speed of light. The excitation rate k_{ex} (unit photons/molecule/s) can be calculated by multiplication of the absorption cross section σ and the photon flux Ψ[43]:

$$k_{ex} = \sigma \Psi \qquad \text{(S3)}$$

The radiative decay rate k_f (unit photons/molecule/s) yielding fluorescence is proportional to k_{ex} and the fluorescence quantum yield according to:

$$k_f = Q \, k_{ex} \qquad \text{(S4)}$$

The rate of photobleaching k_{bl} (units s^{-1}) is given as the fraction of molecules that are photobleached per unit of time. From this the average number of photons a molecule emits before bleaching (N_{em}, units photons/molecule) can be calculated as:

$$N_{em} = \frac{k_f}{k_{bl}} = \frac{1000 \ln 10 \, \varepsilon W Q \lambda}{h c N_A k_{bl}} \qquad \text{(S5)}$$

By substituting $\varepsilon = 30{,}000\ M^{-1} \cdot cm^{-1}$ and $\lambda = 435 \cdot 10^{-9}$ m for CFP molecules, **Equation S5** can be approximated by:

$$N_{em} = \frac{251 W Q}{k_{bl}} \qquad \text{(S6)}$$

From the data provided in **Fig. 6k** and **Supplementary Fig. S9**, N_{em} is calculated at two employed excitation energies for various CFPs and listed in **Supplementary Table S5**.

Supplementary references

37. J. C. Gordon et al., H++: a server for estimating pKas and adding missing hydrogens to macromolecules., *Nucleic Acids Res.* **33**, W368-W371 (2005).

38. T. J. Dolinsky et al., PDB2PQR: expanding and upgrading automated preparation of biomolecular structures for molecular simulations, *Nucleic Acids Res.* **35**, W522-W525 (2005).

39. W. L. Jorgensen, J. Chandrasekhar, J. D. Madura, R. W. Impey, and M. L. Klein, Comparison of simple potential functions for simulating liquid water *J. Chem. Phys.* **79**, 926-935 (1983).

40. G. Vallverdu et al., Relation between pH, structure, and absorption spectrum of Cerulean: a study by molecular dynamics and TD DFT calculations, *Proteins* **78**, 1040-1054 (2010).

41. M. P. Repasky, J. Chandrasekhar, and W. L. Jorgensen, PDDG/PM3 and PDDG/MNDO: improved semiempirical methods, *J. Comput. Chem.* **23**, 1601-1622 (2002).

42. R. Nifosi, P. Amat, and V. Tozzini, Variation of spectral, structural, and vibrational properties within the intrinsically fluorescent proteins family: a density functional study, *J. Comput. Chem.* **28**, 2366-2377 (2007).

43. T. M. Jovin and D. J. Arndt-Jovin, Luminescence digital imaging microscopy, *Annu. Rev. Biophys. Biophys. Chem.* **18**, 271-308 (1989).